Mathematical Biosciences and Engineering

https://www.aimspress.com/journal/mbe

MBE, 23(8): 2287–2306.
DOI: 10.3934/mbe.2026083
Received: 04 March 2026
Revised: 09 June 2026
Accepted: 22 June 2026
Published: 21 July 2026

Research article

Analysis of a mathematical model for fluid transport in poroelastic materials in 2D space

Roman Cherniha[1,*], Vasyl' Davydovych[2], Joanna Stachowska-Pietka[3] and Jacek Waniewski[3]

[1] Department of Mathematics, National University of Kyiv-Mohyla Academy, 2, Skovoroda Street, Kyiv 04070, Ukraine

[2] Institute of Mathematics, NAS of Ukraine, 3, Tereshchenkivs'ka Street, 01004 Kyiv, Ukraine

[3] Institute of Biocybernetics and Biomedical Engineering, PAS, Ks. Trojdena 4, 02 796 Warsaw, Poland

* **Correspondence:** Email: r.m.cherniha@gmail.com.

Abstract: Mathematical models that are based on the poroelastic theory are applied in biology, medicine, and biomedical engineering to describe a wide range of processes. In this work, a mathematical model for poroelastic materials (PEM) with variable volumes is developed in a multidimensional case. Governing equations of the model are constructed using continuity equations, which reflect the well-known physical laws. The deformation vector is specified using the Terzaghi effective stress tensor. In the two-dimensional space case, the model is studied by analytical methods. Using the classical Lie method, it is proven that the relevant nonlinear system of the $(1+2)$-dimensional governing equations admits highly nontrivial Lie symmetries which lead to an infinite-dimensional Lie algebra. The radially-symmetric case is studied in details. It is shown how correct boundary conditions in the case of PEM in the form of a ring and an annulus are constructed. As a result, boundary-value problems with a moving boundary describing the ring (annulus) deformation are constructed. The relevant nonlinear boundary-value problems are analytically solved in the stationary case. In particular, the analytical formulae for unknown deformations and an unknown radius of the annulus are derived. Moreover, illustrative plots for parameters, which are typical for the tumor tissue deformation, are presented.

Keywords: poroelastic material; continuity equations; nonlinear PDE; Lie symmetry; exact solution; steady-state solution

1. Introduction

The modern poroelastic theory is well presented in literature [1–5]. Mathematical models that were created on the basis of this theory are widely applied in geology to describe the penetration of water or oil across soil or cracked rock (see, e.g., [6–8]). Moreover, there are many applications of the poroelastic theory in biology, medicine, and biomedical engineering to describe a wide range of processes (see, e.g., [2, 9–16]).

First, we point out that the poroelastic theory uses several notions (displacement, stress tensor, strain tensor, etc.) from the elasticity theory applied to the materials of continuum mechanics (see, e.g., [17, 18] and papers cited therein). However, in contrast to the elasticity theory, the poroelastic theory considers the system formed by a solid, elastic matrix with pores that can be penetrated by a fluid and dissolved solutes (e.g., water with high concentration of salts). The poroelastic material (PEM) is considered as the superposition of two continious media: the matrix (skeleton) and the system of pores saturated by a fluid. The deformation of the system under the fluid pressure is described by a deformation vector, and the dynamics of the deformation under the forces needs, in general, to be described by second order tensors. The relationship between stress and strain is usually assumed to be linear. The flux of fluid depends on the hydrostatic pressure and fluid (solute, oil) gradients (called osmotic pressure). Additionally, the diffusive and convectivex transport mechanisms should be taking into account.

The general three-dimensional theory describing fluid transport in PEM is very complex because relevant mathematical models involve 3D nonlinear partial differential equations (PDEs). Moreover, if one takes time-dependence into account, then 4D PDEs should be used. As a result, its reduction to two- or one-dimensional version is often discussed [14–16, 19–21]. In particular, the relevant mathematical models can be analytically solved in some cases (at least under some assumptions). In contrast to the above cited papers, here, a multidimensional model is developed and analytical results are derived in the 2D space case. It should be stressed that analytical results, especially exact solutions, do help to understand the role of different parameters and are useful to estimate the accuracy of numerical simulations.

Nowadays, the most powerful methods to construct the exact solutions to nonlinear PDEs are symmetry-based methods, in particular, the Lie method and its generalizations. There are thousands of published papers devoted to the application of symmetry-based methods to PDEs; therefore, we list only some recent monographs, such as [22–24]. It should be pointed out that the authors typically examine scalar PDEs because the search for symmetries of *systems of nonlinear PDEs* is a much complicated problem. In fact, essential technical difficulties occur if one intends to identify symmetries and construct exact solutions for systems of PDEs. A typical example is the very recent study [25], in which the authors considered a three-component system arising in fluid dynamics for the very beginning. However, in order to identify symmetries, they simplified the system to a single fourth-order PDE and were only able to obtain particular results about symmetries of the PDE in question [26]. There are some rigorous studies devoted to the application of symmetry-based methods to systems of nonlinear PDEs, in particular, the papers devoted to *multicomponent systems of PDEs* (notably, the model developed below is such a system). Taking the above observation into account, we refer the reader to the recent works [27–32], which are devoted to applications of symmetry-based methods to the nonlinear multicomponent systems of PDEs.

This work is organized as follows. In Section 2, a mathematical model for PEM with variable volumes is developed in a multidimensional case. Governing equations of the model are constructed using the continuity equations, which reflect the well-known physical laws. The deformation vector is specified using the Terzaghi effective stress tensor (see, e.g., [2, 5, 33]). In Section 3, the model is studied in the 2D space approximation. Using the classical Lie method, we prove that the governing equations, which form a six-component system of nonlinear (1 + 2)-dimensional PDEs, admit highly nontrivial Lie symmetries, which lead to infinite-dimensional Lie algebra. In Section 4, the radially-symmetric case is studied. It is shown how correct boundary conditions are constructed in the case of PEM in the form of a ring that is shrinking. As a result, the boundary-value problem (BVP) with a moving boundary describing the ring (annulus) deformation is constructed. In Section 5, the nonlinear BVP obtained in the previous section is analytically solved in the stationary case. It is shown how deformation and an unknown radius of PEM after shrinking can be exactly calculated by relevant formulae. Illustrative plots are presented for the parameters, which are typical for the tumor tissue deformation. Finally, we discuss the results obtained and present some conclusions in the last section.

2. A model for fluid and solute transport in PEM

The mathematical model for PEM with variable volumes is developed under the following assumptions:

(1) PEM consists of pores and matrix;
(2) no internal sources/sinks;
(3) deformation is described by a linear stress tensor;
(4) incompressible fluid;
(5) isothermal conditions for transport in PEM.

The governing equations of the model consist of continuity equations.

Let us consider an infinitesimal element dV of PEM without division on two phases. The volume balance is as follows (see Chapter 10 in [2] and [16]):

$$\frac{1}{dV}\frac{\partial(dV)}{\partial t} = \frac{\partial e}{\partial t} = \frac{\partial \nabla \cdot \bar{u}}{\partial t} = -\nabla \cdot \bar{j}_V. \tag{2.1}$$

Here, the deformation vector u is defined as follows:

$$u(\bar{x}, t; \bar{X}) = \bar{x}(t) - \bar{X},\ \bar{X} = \bar{x}\,(0)\,, \quad e = \nabla \cdot \bar{u}, \tag{2.2}$$

where $\bar{j}_V$ is the volumetric flux across the PEM (will be determined later), $\bar{X} = (X_1, \ldots, X_n)$ is the initial position within PEM, and $\bar{x}(t) = (x_1(t), \ldots, x_n(t))$ is the position at time t (i.e., after displacement (deformation)).

Consider the mass ρdV of the infinitesimal element dV. The mass conservation law gives the following continuity equation:

$$\frac{1}{dV}\frac{\partial\,(\rho dV)}{\partial t} = \frac{\partial \rho}{\partial t} + \rho\frac{\partial e}{\partial t} = -\nabla \cdot \bar{j}_\rho.$$

Thus,

$$\frac{\partial \rho}{\partial t} = -\nabla \cdot \bar{j}_\rho + \rho\nabla \cdot \bar{j}_V, \tag{2.3}$$

where $\bar{j}_\rho$ is the flux of mass through the PEM (will be determined later).

On the other hand, one may consider the infinitesimal element dV as a PEM element consisting of the fluid phase F with the fractional volume (porosity) θ_F and the density ρ_F, and the solid (matrix) phase M with the fractional volume θ_M and the density ρ_M. Obviously,

$$\rho = \rho_F\theta_F + \rho_M\theta_M, \quad \theta_F + \theta_M = 1, \tag{2.4}$$

with $\rho_F = \rho_F^0 = const$ (incompressibility).

The volume balance equations are

$$\frac{1}{dV}\frac{\partial(\theta_F dV)}{\partial t} = \frac{\partial\theta_F}{\partial t} + \theta_F\frac{\partial e}{\partial t} = -\nabla\cdot\bar{j}_{VF},$$

$$\frac{1}{dV}\frac{\partial(\theta_M dV)}{\partial t} = \frac{\partial\theta_M}{\partial t} + \theta_M\frac{\partial e}{\partial t} = -\nabla\cdot\bar{j}_{VM},$$

so that

$$\frac{\partial\theta_F}{\partial t} = -\nabla\cdot\bar{j}_{VF} + \theta_F\nabla\cdot\bar{j}_V, \tag{2.5}$$

$$\frac{\partial\theta_M}{\partial t} = -\nabla\cdot\bar{j}_{VM} + \theta_M\nabla\cdot\bar{j}_V, \tag{2.6}$$

where $\bar{j}_{VF}$ is the volumetric flux in the fluid phase (will be determined later), and $\bar{j}_{VM}$ is the volumetric flux in the matrix phase (will be determined later).

The mass conservation law gives the following equations for each phase:

$$\frac{1}{dV}\frac{\partial(\rho_F\theta_F dV)}{\partial t} = \frac{\partial(\rho_F\theta_F)}{\partial t} + \rho_F\theta_F\frac{\partial e}{\partial t} = -\nabla\cdot\left(\rho_F\bar{j}_{VF}\right), \tag{2.7}$$

$$\frac{1}{dV}\frac{\partial(\rho_M\theta_M dV)}{\partial t} = \frac{\partial(\rho_M\theta_M)}{\partial t} + \rho_M\theta_M\frac{\partial e}{\partial t} = -\nabla\cdot\left(\rho_M\bar{j}_{VM}\right). \tag{2.8}$$

Since we assume that the fluid phase is a solution (not pure water) with the concentration $c(t,x)$ (e.g., glucose molecules), the corresponding continuity equation can be written as follows:

$$\frac{1}{dV}\frac{\partial(c\theta_F dV)}{\partial t} = \frac{\partial(c\theta_F)}{\partial t} + c\theta_F\frac{\partial e}{\partial t} = -\nabla\cdot\bar{j}_S, \tag{2.9}$$

where $\bar{j}_S$ is the solute flux across the PEM.

Because the PEM is deformed with time, the dynamics of the PEM element of the mass ρdV with the velocity $\frac{\partial u}{\partial t}$ can be described by the Newton law as follows:

$$\frac{1}{dV}\frac{\partial\left(\rho\frac{\partial u}{\partial t}dV\right)}{\partial t} = \rho\frac{\partial^2 u}{\partial t^2} + \frac{\partial u}{\partial t}\left(\frac{\partial\rho}{\partial t} + \rho\frac{\partial e}{\partial t}\right) = \nabla\cdot\tilde{\tau}, \tag{2.10}$$

where $\tilde{\tau}$ is an effective stress tensor. In the general case, $\tilde{\tau}$ should be the Cauchy effective stress tensor with possible nonlinear terms w.r.t. the dilatation $e = \nabla\cdot\bar{u}$ [5]. However, if we restrict ourselves to the linear poroelastic theory for isotropic materials, then it is the Terzaghi effective stress tensor (see, e.g., [2, 5, 33])

$$\tilde{\tau}_t = -p^*I + E\varepsilon = -p^*I + \lambda Tr\varepsilon I + 2\mu\varepsilon. \tag{2.11}$$

Here, $p^* = p - \sigma_1 c$ is the effective pressure given by the difference between hydrostatic pressure and osmotic pressure, σ_1 is a constant parameter (see below for more details), λ and μ are the Lame coefficients, and ε represents the strain tensor in the form of the symmetric matrix $n \times n$; in particular, for $n = 2$,

$$\varepsilon = \frac{1}{2}\left(\nabla\bar{u} + \nabla\bar{u}^T\right) = \begin{pmatrix} u_x^1 & \frac{1}{2}(u_y^1 + u_x^2) \\ \frac{1}{2}(u_y^1 + u_x^2) & u_y^2 \end{pmatrix}.$$

Remark 2.1. In the case of anisotropic materials, the matrix $\tilde{\tau}_t$ has a more complicated structure which can be found (e.g., in [2]).

In order to obtain a closed system of PDEs for finding unknown functions, one needs to specify the fluxes across the PEM.

In the fluid phase, we have the following flux:

$$\bar{j}_{VF} = \theta_F \frac{\partial \bar{u}}{\partial t} - k\nabla \cdot p^* \equiv \theta_F \frac{\partial \bar{u}}{\partial t} - k\left(\nabla p - \sigma_1 \nabla c\right).$$

Here, the first term means the deformation contribution, and the second is the volumetric fluid flux relative to the matrix calculated according to the extended Darcy's law with hydraulic conductivity k.

The volumetric flux in the solid phase (matrix) is as follows :

$$\bar{j}_{VM} = \theta_M \frac{\partial \bar{u}}{\partial t}.$$

In contrast to the fluxes defined above, the solute flux through the PEM includes the diffusive term reflecting Fick's law, and the convective term as follows:

$$\bar{j}_S = -D\nabla c + S c \bar{j}_{VF},$$

i.e.,

$$\bar{j}_S = -D\nabla c - Skc(\nabla p - \sigma_1 \nabla c) + \theta_F c \frac{\partial \bar{u}}{\partial t},$$

where D is the solute diffusivity, and $S < 1$ is the so-called sieving coefficient of the solute in the PEM. In the case of homogeneous membranes, which can be considered as PEM, the coefficient $S = 1 - \sigma$, where $\sigma < 1$ is the reflection coefficient (see, e.g., [34]). The latter is related to the osmotic pressure and it can be identified that $\sigma_1 = \sigma RT$, where R is the gas constant and T is a given temperature.

Finally, if you go back to the continuity equations (2.1) and (2.3), the fluxes $\bar{j}_V$ and $\bar{j}_\rho$ should be related to the above defined fluxes as follows:

$$\bar{j}_V = \bar{j}_{VF} + \bar{j}_{VM} = -k(\nabla p - \sigma_1 \nabla c) + \frac{\partial u}{\partial t},$$

$$\bar{j}_\rho = \rho_F \bar{j}_{VF} + \rho_M \bar{j}_{VM} = -k\rho_F(\nabla p - \sigma_1 \nabla c) + \rho \frac{\partial u}{\partial t}.$$

Now, one realizes that Eqs (2.1) and (2.3) are algebraic consequences of Eqs (2.5)–(2.8) written down for each phase of PEM; therefore, those can be skipped.

Thus, by inserting the fluxes defined above into the governing equations (2.5)–(2.10) and making the relevant transformations and calculations, one arrives at a system of $n + 4$ PDEs for unknown functions $\bar{u} = (u_1, \ldots, u_n)$, θ_F, ρ, c, and p. Two other unknown functions, ρ_M and θ_M, are defined by the algebraic equations (2.4).

In the case of the 1D approximation ($n = 1$), the system obtained was studied in [14, 16]. The rest of this study is devoted to the case when $n = 2$.

3. The 2D model and its Lie symmetry

In the 2D space approximation, the governing equations of the model possess the following form:

$$2\nabla \cdot \bar{u}_t = k\Delta p^*, \tag{3.1}$$

$$\rho u^1_{tt} + u^1_t(\rho_t + \rho\nabla \cdot \bar{u}_t) = \lambda^* u^1_{xx} + \mu u^1_{yy} + (\lambda^* - \mu)u^2_{xy} - p^*_x, \tag{3.2}$$

$$\rho u^2_{tt} + u^2_t(\rho_t + \rho\nabla \cdot \bar{u}_t) = \lambda^* u^2_{yy} + \mu u^2_{xx} + (\lambda^* - \mu)u^1_{xy} - p^*_y, \tag{3.3}$$

$$\rho_t + \bar{u}_t\nabla\rho = k(\rho^0_F - \rho)\Delta p^*, \tag{3.4}$$

$$\theta_{Ft} + \bar{u}_t\nabla\theta_F = k(1 - \theta_F)\Delta p^*, \tag{3.5}$$

$$(c\theta_F)_t + \bar{u}_t \cdot \nabla(c\theta_F) = D\Delta c + k(S - \theta_F)c\Delta p^* + kS\nabla c \cdot \nabla p^*, \tag{3.6}$$

where $p^* = p - \sigma_1 c,\ \lambda^* = \lambda + 2\mu$, Δ is the Laplace operator, $\nabla \cdot \bar{f} \equiv f^1_x + f^2_y$, and the lower subscripts t and x denote differentiation with respect to these variables. Natural restrictions on the parameters arising above are as follows:

$$k > 0,\ D > 0,\ \rho^0_F > 0,\ 0 < S < 1,\ \lambda > 0,\ \mu > 0. \tag{3.7}$$

Remark 3.1. Generally speaking, some limiting cases may occur when some parameters vanish. For example, $D \simeq 0$ when very large molecules (e.g., albumin) are dissolved in the fluid. Here, we do not consider such limiting cases.

We remind the reader that the above equations were derived under the assumption that the PEM is an isotropic material. If this assumption is removed, then the Terzaghi effective stress tensor (2.11) is more complicated and reads as follows:

$$\tilde{\tau}_{ter} = -p^* I + E\epsilon, \tag{3.8}$$

with the symmetric matrix [2]

$$E = \begin{pmatrix} E_{11} & E_{12} & \sqrt{2}E_{13} \\ E_{12} & E_{22} & \sqrt{2}E_{23} \\ \sqrt{2}E_{13} & \sqrt{2}E_{23} & 2E_{33} \end{pmatrix} \tag{3.9}$$

and the strain tensor

$$\epsilon = \frac{1}{2}\left(\nabla\bar{u} + \nabla\bar{u}^T\right) \Leftrightarrow \left(u^1_x, u^2_y, \frac{\sqrt{2}}{2}(u^1_y + u^2_x)\right)^T. \tag{3.10}$$

Here, $E_{ii} > 0,\ E_{ij} \geq 0, i \neq j$.

Remark 3.2. In the case of isotropic materials, the above matrix essentially simplifies because

$$E_{13} = E_{23} = 0,\ E_{33} = \mu,\ E_{11} = E_{22} = \lambda + 2\mu,\ E_{12} = E_{22} - 2E_{33} = \lambda, \tag{3.11}$$

where λ and μ are the Lame coefficients.

Thus, making a similar routine as the aforementioned isotropic case, the governing equations for the fluid and solute transport in the PEM can be derived in the following anisotropic case:

$$
\begin{aligned}
& u^1_{tx} + u^2_{ty} = \tfrac{k}{2}\Delta p^*, \\
& (\rho_t + \rho(u^1_{tx} + u^2_{ty}))u^1_t + \rho u^1_{tt} = \\
& \qquad -p^*_x + E_{11}u^1_{xx} + E_{33}u^1_{yy} + E_{13}u^2_{xx} + E_{23}u^2_{yy} + 2E_{13}u^1_{xy} + (E_{12} + E_{33})u^2_{xy}, \\
& (\rho_t + \rho(u^1_{tx} + u^2_{ty}))u^2_t + \rho u^2_{tt} = \\
& \qquad -p^*_y + E_{22}u^2_{yy} + E_{33}u^2_{xx} + E_{13}u^1_{xx} + E_{23}u^1_{yy} + 2E_{23}u^2_{xy} + (E_{12} + E_{33})u^1_{xy}, \\
& \rho_t + \rho_x u^1_t + \rho_y u^2_t = k(\rho^0_F - \rho)\Delta p^* \\
& \theta_{F\,t} + \theta_{F\,x}u^1_t + \theta_{F\,y}u^2_t = k\,(1 - \theta_F)\,\Delta p^*, \\
& (c\theta_F)_t + (c\theta_F)_x\, u^1_t + (c\theta_F)_y\, u^2_t = D\Delta c + k(S - \theta_F)c\Delta p^* + kS\,\nabla c \cdot \nabla p^*.
\end{aligned}
\tag{3.12}
$$

In the case of isotropic PEM, the governing equation (3.12) coincide with the PDE systems (3.1)–(3.6).

Theorem 3.3. *The nonlinear PDE system (3.12) is invariant w.r.t. an infinitely-dimensional Lie algebra. By assuming that all parameters are arbitrary, the Lie algebra is generated by the Lie symmetry operators as follows:*

$$
\begin{aligned}
& \tfrac{\partial}{\partial t},\ \tfrac{\partial}{\partial x},\ \tfrac{\partial}{\partial y},\ c\tfrac{\partial}{\partial c}, \\
& g(t)\tfrac{\partial}{\partial p^*},\ G^1(x,y)\tfrac{\partial}{\partial u^1} + G^2(x,y)\tfrac{\partial}{\partial u^2}.
\end{aligned}
\tag{3.13}
$$

Here, $g(t)$ is an arbitrary function, while the functions $G^i,\ i = 1,2$ form an arbitrary solution of the linear PDE system as follows:

$$
\begin{aligned}
& E_{11}G^1_{xx} + E_{33}G^1_{yy} + E_{13}G^2_{xx} + E_{23}G^2_{yy} + 2E_{13}G^1_{xy} + (E_{12} + E_{33})G^2_{xy} = 0, \\
& E_{22}G^2_{yy} + E_{33}G^2_{xx} + E_{13}G^1_{xx} + E_{23}G^1_{yy} + 2E_{23}G^2_{xy} + (E_{12} + E_{33})G^1_{xy} = 0.
\end{aligned}
$$

Depending on the parameters E_{ij}, there is only a single extension of the principal algebra (3.13). Thus, the extension only occurs under the conditions (3.11) (i.e., in the case of isotropic PEM).

Theorem 3.4. *The nonlinear PDE systems (3.1)–(3.6) is invariant w.r.t. an infinitely-dimensional Lie algebra. By assuming that all parameters are arbitrary, the Lie algebra is generated by the Lie symmetry operators as follows:*

$$
\begin{aligned}
& \tfrac{\partial}{\partial t},\ \tfrac{\partial}{\partial x},\ \tfrac{\partial}{\partial y},\ c\tfrac{\partial}{\partial c}, \\
& g(t)\tfrac{\partial}{\partial p^*},\ G^1(x,y)\tfrac{\partial}{\partial u^1} + G^2(x,y)\tfrac{\partial}{\partial u^2}, \\
& y\tfrac{\partial}{\partial x} - x\tfrac{\partial}{\partial y} + u^2\tfrac{\partial}{\partial u^1} - u^1\tfrac{\partial}{\partial u^2}.
\end{aligned}
$$

Here, the functions $G^i,\ i = 1,2$ form an arbitrary solution of the linear PDE system as follows:

$$
\begin{aligned}
& \lambda^* G^1_{xx} + \mu G^1_{yy} + (\lambda^* - \mu)G^2_{xy} = 0, \\
& \mu G^2_{xx} + \lambda^* G^2_{yy} + (\lambda^* - \mu)G^1_{xy} = 0.
\end{aligned}
\tag{3.14}
$$

Sketch of the proof of Theorems 3.3 and 3.4. The proof is based on the Lie infinitesimal invariance criterion (see, e.g., Section 1.2.5 [22]). Since the PDE system (3.12) only contains constant parameters (i.e., one does not involve arbitrary functions), the problem of Lie symmetry classification is a mostly technical routine. It mainly involves cumbersome calculations due to the detailed examination of the determining equations under restrictions (3.7) and $E_{ii} > 0,\ E_{ij} \geq 0, i \neq j$. The process requires careful attention to the restrictions and the step-by-step calculation of all possible symmetries. This process is omitted here; however, we refer interested readers to the recent study [19], in which nonlinear PDE systems (3.1)–(3.6) in 1D space case is studied and the relevant details for the Lie symmetry search are presented. Notably, the computer algebra package Maple was unable to calculate Lie symmetries of PDE systems (3.12) and (3.1)–(3.6).

Remark 3.5. The PDE system (3.14) is reducible to the system of the first-order PDEs

$$\begin{aligned} \lambda^* F^1_x - \mu F^2_y = 0, \\ \lambda^* F^1_y + \mu F^2_x = 0, \end{aligned} \tag{3.15}$$

by the substitution

$$F^1(x, y) = G^1_x + G^2_y,\ F^2(t, x) = G^2_x - G^1_y.$$

System (3.15) has the following solution:

$$F^1 = \mu \left(f_1(x + iy) + i f_2(x - iy) \right),\ F^2 = -\lambda^* \left(i f_1(x + iy) + f_2(x - iy) \right),$$

where f_1 and f_2 are arbitrary functions, and $i = \sqrt{-1}$. Notably, (3.15) is nothing else but the well-known Cauchy–Riemann system in a non-standard form.

According to the Lie continuous groups theory, the Lie symmetry operator

$$y\frac{\partial}{\partial x} - x\frac{\partial}{\partial y} + u^2\frac{\partial}{\partial u^1} - u^1\frac{\partial}{\partial u^2} \tag{3.16}$$

generates the one-parameter Lie group

$$(x', y')^T = A(x, y)^T, \quad ((u^1)', (u^2)')^T = A(u^1, u^2)^T,$$

where $A = \begin{pmatrix} \cos\phi & -\sin\phi \\ \sin\phi & \cos\phi \end{pmatrix}$ is a rotation matrix, and ϕ is a group parameter. Thus, the above Lie symmetry reflects invariance of the system w.r.t. rotations. Interestingly, the Lie symmetry (3.16) has the same form as for the classical Navier–Stokes equations (in 2D approximation) [35] and a tumor growth model that was studied in [36].

4. The radially-symmetric case

Here, we are looking for solutions with radial symmetry of the governing equations (3.1)–(3.6), which are predicted by the Lie symmetry (3.16). Thus, one can rewrite the system in polar coordinates, using the following transformations:

$$\begin{aligned} & x = r\cos\phi,\ y = r\sin\phi, \\ & u^1 = w^1\cos\phi - w^2\sin\phi,\ u^2 = w^1\sin\phi + w^2\cos\phi, \\ & p = P(t, r, \phi),\ \rho = \varrho(t, r, \phi),\ \theta_F = \Theta(t, r, \phi),\ c = C(t, r, \phi), \end{aligned} \tag{4.1}$$

which are typically used for the displacement vector (u^1, u^2) (see, e.g., [2]).

By applying transformation (4.1) to the governing equations (3.1)–(3.6), we arrive at the following system:

$$
\begin{aligned}
&\left(\left(rw^1\right)_r + w^2_\phi\right)_t = \tfrac{k}{2r}\, P_{\phi\phi} + \tfrac{k}{2}\, (rP_r)_r\,, \\
&w^1_t \left(\varrho_t + \varrho w^1_{tr} + \tfrac{1}{r}\varrho w^1_t + \tfrac{1}{r}\varrho w^2_{t\phi}\right) + \varrho w^1_{tt} = -P_r + \lambda^* w^1_{rr} + \tfrac{\lambda^*}{r}\, w^1_r - \tfrac{\lambda^*}{r^2}\, w^1 + \\
&\qquad\qquad \tfrac{1}{r^2}\left((\lambda^* - \mu) r w^2_{r\phi} + \mu w^1_{\phi\phi} - (\lambda^* + \mu) w^2_\phi\right), \\
&w^2_t \left(\varrho_t + \varrho w^1_{tr} + \tfrac{1}{r}\varrho w^1_t + \tfrac{1}{r}\varrho w^2_{t\phi}\right) + \varrho w^2_{tt} = -\tfrac{1}{r} P_\phi + \mu w^2_{rr} + \tfrac{\mu}{r}\, w^2_r - \tfrac{\mu}{r^2}\, w^2 + \\
&\qquad\qquad \tfrac{1}{r^2}\left((\lambda^* - \mu) r w^1_{r\phi} + \lambda^* w^2_{\phi\phi} + (\lambda^* + \mu) w^1_\phi\right), \\
&r\varrho_t + r\varrho_r w^1_t + \varrho_\phi w^2_t = k(\rho^0_F - \varrho)\left(\tfrac{P_{\phi\phi}}{r} + (rP_r)_r\right), \\
&r\Theta_t + r\Theta_r w^1_t + \Theta_\phi w^2_t = k(1 - \Theta)\left(\tfrac{P_{\phi\phi}}{r} + (rP_r)_r\right), \\
&r\,(C\Theta)_t + r\,(C\Theta)_r\, w^1_t + (C\Theta)_\phi\, w^2_t = \\
&\qquad\qquad D\left(\tfrac{C_{\phi\phi}}{r} + (rC_r)_r\right) + k(S - \Theta)C\left(\tfrac{P_{\phi\phi}}{r} + (rP_r)_r\right) + \tfrac{kS}{r}\left(C_\phi P_\phi + r^2 C_r P_r\right).
\end{aligned}
\tag{4.2}
$$

Simultaneously, the Lie symmetry (3.16) essentially takes the simpler form

$$J = -\partial_\phi. \tag{4.3}$$

The relevant ansatz generated by operator (4.3) leads to exact solutions with radial symmetry and has the form

$$
\begin{aligned}
&w^1 = w^1(t, r),\ w^2 = w^2(t, r),\ P = P(t, r), \\
&\varrho = \varrho(t, r),\ \Theta = \Theta(t, r),\ C = C(t, r).
\end{aligned}
\tag{4.4}
$$

By substituting ansatz (4.4) into (4.2), one obtains the following system of $(1 + 1)$-dimensional equations:

$$
\begin{aligned}
&\left(rw^1\right)_{rt} = \tfrac{k}{2}\, (rP_r)_r\,, \\
&w^1_t \left(\varrho_t + \varrho w^1_{tr} + \tfrac{1}{r}\varrho w^1_t\right) + \varrho w^1_{tt} = -P_r + \lambda^* w^1_{rr} + \tfrac{\lambda^*}{r}\, w^1_r - \tfrac{\lambda^*}{r^2}\, w^1, \\
&w^2_t \left(\varrho_t + \varrho w^1_{tr} + \tfrac{1}{r}\varrho w^1_t\right) + \varrho w^2_{tt} = \mu w^2_{rr} + \tfrac{\mu}{r}\, w^2_r - \tfrac{\mu}{r^2}\, w^2, \\
&r\varrho_t + r\varrho_r w^1_t = k(\rho^0_F - \varrho)\,(rP_r)_r\,, \\
&r\Theta_t + r\Theta_r w^1_t = k(1 - \Theta)\,(rP_r)_r\,, \\
&r\,(C\Theta)_t + r\,(C\Theta)_r\, w^1_t = D\,(rC_r)_r + k(S - \Theta)C\,(rP_r)_r + kS\ rC_r P_r.
\end{aligned}
\tag{4.5}
$$

Example. Let us consider the PEM in the form of a circle (ring) with a radius R_0 (see Figure 1). We assume that all pores in the circle are connected by capillaries/fibers (this is not shown on the picture), saturated by water, and the system is in steady-state (the gravity force is not taken into account). At the time moment $t = 0$, a load F_0 begins to shrink (squeeze) the circle in the radially-symmetric direction. As a result, the boundary of the circle starts to move and simultaneously one expects a water outflow throughout the moving boundary. In the porous circle, the diffusion process of the water towards the boundary takes place. At the time moment $t = T$, the load stops to act. Finally, one obtains a new porous circle with a radius $r_{st} < R_0$. In the new steady-state, the porosity of the circle will be smaller because we assume a constant pressure p_a at the ring surface all time; however, the matrix volume (actually it is the square) is still the same as at the moment $t = 0$.

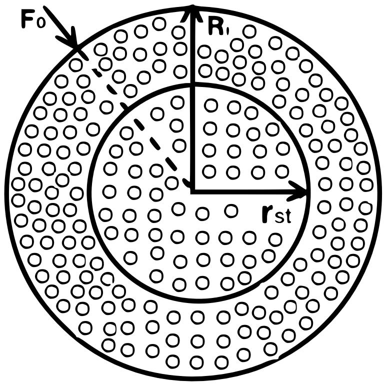

Figure 1. PEM in the form of a circle (ring) with the initial radius R_1 and the radius r_{st} after deformation caused by the load F_0.

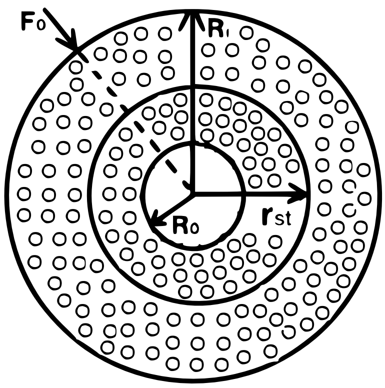

Figure 2. PEM in the form of an annulus with the initial outer radius R_1 and the radius r_{st} after deformation caused by the load F_0.

The process described above allow us to simplify the governing equation (4.2). In fact, deformation will only take place in the radially-symmetric direction, while the tangential deformation is zero (or negligibly small); therefore, one may set $w^2 = 0$ (i.e., the third equation in (4.5) vanishes). Moreover, we consider pure water (i.e., there is no solute transport); therefore, the last equation can be skipped because one may set $C = 0$. As a result, the mathematical model that describes the deformation of the

PEM in the form of the circle consists of the following governing equations:

$$\begin{aligned}
&w_{tr} + \tfrac{1}{r} w_t = \tfrac{k}{2}\left(P_{rr} + \tfrac{1}{r} P_r\right), \\
&w_t\left(\varrho_t + \varrho w_{tr} + \tfrac{1}{r}\varrho w_t\right) + \varrho w_{tt} = -P_r + \lambda^* w_{rr} + \tfrac{\lambda^*}{r} w_r - \tfrac{\lambda^*}{r^2} w, \\
&\varrho_t + \varrho_r w_t = k(\rho_F^0 - \varrho)\left(P_{rr} + \tfrac{1}{r} P_r\right), \\
&\Theta_t + \Theta_r w_t = k\,(1 - \Theta)\left(P_{rr} + \tfrac{1}{r} P_r\right),
\end{aligned} \tag{4.6}$$

where the notation $w = w^1$ is used.

In order to complete the mathematical model, one needs to specify boundary conditions and initial profiles.

The boundary conditions are as follows:

$$\begin{aligned}
&r = 0: \quad \tfrac{\partial P}{\partial r} = 0,\ \tfrac{\partial \varrho}{\partial r} = 0,\ \tfrac{\partial \Theta}{\partial r} = 0,\ w = 0, \\
&r = S(t): \quad P = p_a,\ w = S(t) - R_0,
\end{aligned} \tag{4.7}$$

where $S(t)$ is an unknown function that essentially depends on the load F_0 and has the specified values $S(0) = R_0$ and $S(T) = r_{st}$.

The initial conditions are as follows:

$$t = 0: \quad P = p_a,\ \varrho = \varrho_0(r),\ \Theta = \Theta_0(r),\ w = 0, \tag{4.8}$$

and the condition for the final displacement of the surface is

$$t = T: \quad w = r_{st} - R_0, \tag{4.9}$$

where $\varrho_0(r)$ and $\Theta_0(r) < 1$ are given positive functions, and R_0 and r_{st} are known positive constants.

In order to take the load F_0 (generally speaking, it can be a function of time and space) acting on the moving boundary into account, we need to specify the Terzaghi effective stress tensor in the radially-symmetric case. Taking the assumption about radial symmetry and the strain tensor matrix presented in [1] (see Appendix A) in the cylindrical coordinates into account, the matrix ε (see (3.10)) is equivalent to the vector

$$\left(\frac{\partial w}{\partial r}, \frac{w}{r}, 0\right)^T.$$

Thus, using formulae (3.8), (3.9) and (3.11), the Terzaghi effective stress tensor can be derived in the form

$$\left(-P + \lambda^* \frac{\partial w}{\partial r} + \frac{\lambda}{r} w, -P + \lambda \frac{\partial w}{\partial r} + \frac{\lambda^*}{r} w, 0\right)^T.$$

It means that the tensor matrix $\tilde{\tau}_{ter}$ is a diagonal matrix with the nonzero elements

$$\tau_{11} = -P + \lambda^* \frac{\partial w}{\partial r} + \frac{\lambda}{r} w, \quad \tau_{22} = -P + \lambda \frac{\partial w}{\partial r} + \frac{\lambda^*}{r} w.$$

Because the load F_0 only pushes the boundary along the radius r, one readily obtains the condition $\tilde{\tau}_{ter}\bar{n} = (\tau_{11}, \tau_{22}) \cdot (1, 0) = -\frac{F_0}{2\pi r}$, where $\bar{n} = (1, 0)$ is normal to the boundary. Thus, we arrive at the following additional boundary condition:

$$r = S(t): \quad \lambda^* \frac{\partial w}{\partial r} + \frac{\lambda}{r} w = p_a - \frac{F_0}{2\pi r}. \tag{4.10}$$

Thus, we obtain the BVP with moving boundary that consists of the governing equation (4.6), the boundary conditions (4.7) and (4.10), and the initial conditions (4.8) and (4.9).

The above example can be generalized by replacing the circle by the annulus (see Figure 2) as follows:

$$\Omega = \{(r, \phi): \ R_0 < r < R_1; 0 \le \phi < 2\pi\}.$$

In this case, we may assume the Dirichlet conditions on the interior boundary of the annulus as follows:

$$r = R_0: \quad P = p_a, \ \varrho = \varrho_0, \ \Theta = \Theta_0, \ w = 0. \tag{4.11}$$

The last condition in (4.11) means that the interior of the annulus is fixed (i.e., zero displacement at $r = R_0$).

Remark 4.1. A simpler example for a water-saturated soil layer is studied in [5] (see Chapter 5). The bone deformation was studied in [20] using the bone layer in the form of circle; however, the authors did not present the mathematical model in detail.

5. Stationary exact solution

Constructing the exact solution of the nonlinear BVP that was formulated above is a highly nontrivial problem. Here, we consider the stationary case that can be treated in a straightforward way. In the stationary case (i.e., all unknown functions do not depend on the time variable), the nonlinear system (4.6) reduces to two linear second-order ODEs with the general solution

$$P = P_0 + C_0 \ln r, \quad w = \frac{C_0}{2\lambda^*} r \ln r + C_1 r + C_{-1} r^{-1},$$

while $\varrho(r)$ and $\Theta(r)$ are arbitrary smooth functions (P_0 and C with indices are arbitrary constants).

Let us consider the above example for the PEM in the form of the annulus Ω. The stationary solution satisfies the boundary conditions (4.11) if the following hold:

$$\begin{aligned} &p_a = P_0 + C_0 \ln R_0 \ \Leftrightarrow \ C_0 = \tfrac{p_a - P_0}{\ln R_0}, \\ &\tfrac{p_a - P_0}{2\lambda^*} R_0 + C_1 R_0 + C_{-1} R_0^{-1} = 0 \ \Leftrightarrow \ C_{-1} = \left(\tfrac{P_0 - p_a}{2\lambda^*} - C_1\right) R_0^2. \end{aligned}$$

Let us assume that we have a steady-state (stationary) position of the annulus with the following boundary conditions:

$$r = r_{st}: \ P = p_{st}, \ w = r_{st} - R_1. \tag{5.1}$$

Thus, using the above boundary conditions, we specify P_0 and C_1 as follows:

$$P_0 + \frac{p_a - P_0}{\ln R_0} \ln r_{st} = p_{st} \ \Leftrightarrow \ P_0 = \frac{p_{st} \ln R_0 - p_a \ln r_{st}}{\ln R_0 - \ln r_{st}}, \ r_{st} \ne R_0.$$

In the case $r_{st} = R_0$, the condition $p_{st} = p_a$ takes place. From the second condition in (5.1)

$$\frac{p_a - P_0}{2\lambda^* \ln R_0} r_{st} \ln r_{st} - \frac{(P_0 - p_a)R_0^2}{2\lambda^* r_{st}} + C_1 r_{st} + \left(\frac{P_0 - p_a}{2\lambda^*} - C_1\right)\frac{R_0^2}{r_{st}} = r_{st} - R_1,$$

one defines

$$C_1 = \left(\frac{P_0 - p_a}{2\lambda^* \ln R_0} r_{st} \ln r_{st} - \frac{P_0 - p_a}{2\lambda^*}\frac{R_0^2}{r_{st}} + r_{st} - R_1\right)\frac{r_{st}}{r_{st}^2 - R_0^2},$$

where $r_{st} \neq R_0$.

If $r_{st} = R_0$, then $r_{st} = R_1$, and C_1 is an arbitrary constant; therefore, we arrive at an unrealistic situation where $r_{st} = R_1 = R_0$ (i.e., the annulus degenerates into a circle).

Thus,

$$\begin{aligned} P &= P_0 + (p_a - P_0)\tfrac{\ln r}{\ln R_0}, \\ w &= \tfrac{p_a - P_0}{2\lambda^*} r \tfrac{\ln r}{\ln R_0} + C_1 r + \left(\tfrac{P_0 - p_a}{2\lambda^*} - C_1\right)\tfrac{R_0^2}{r}, \end{aligned} \tag{5.2}$$

where

$$P_0 = \frac{p_{st} \ln R_0 - p_a \ln r_{st}}{\ln R_0 - \ln r_{st}} = p_a + \frac{p_{st} - p_a}{1 - \frac{\ln r_{st}}{\ln R_0}}, \tag{5.3}$$

$$C_1 = \left(\frac{p_{st} - p_a}{2\lambda^*(\ln R_0 - \ln r_{st})}\left(r_{st} \ln r_{st} - \frac{R_0^2 \ln R_0}{r_{st}}\right) + r_{st} - R_1\right)\frac{r_{st}}{r_{st}^2 - R_0^2}.$$

By substituting (5.3) into (5.2), we arrive at the following:

$$\begin{aligned} P &= \tfrac{p_{st} \ln R_0 - p_a \ln r_{st}}{\ln R_0 - \ln r_{st}} - \tfrac{p_{st} - p_a}{\ln R_0 - \ln r_{st}} \ln r, \\ w &= \tfrac{1}{2\lambda^*}\tfrac{p_{st} - p_a}{\ln R_0 - \ln r_{st}}\left(\tfrac{R_0^2}{r} \ln R_0 - r \ln r\right) + C_1\left(r - \tfrac{R_0^2}{r}\right), \end{aligned} \tag{5.4}$$

where $r_{st} \neq R_0$.

Finally, we need to determine the parameter r_{st} that is an analogue of the unknown function $S(t)$ in the nonstationary case. This can be done using a modification of the boundary condition (4.10) in the following form:

$$r = r_{st}: \quad \lambda^* \frac{\partial w}{\partial r} + \frac{\lambda}{r} w = p_a - \frac{F_0(r)}{2\pi r}. \tag{5.5}$$

By substituting the function w from (5.4) into (5.5), one obtains a cumbersome transcendent equation to find r_{st} that is omitted here.

A simpler situation occurs if one applies the boundary conditions that involve the Neumann condition (zero flux) for the pressure P:

$$r = R_0: \ \frac{\partial P}{\partial r} = 0, \ w = 0.$$

The above conditions immediately produce the following:

$$\left.\frac{\partial P}{\partial r}\right|_{r=R_0} = \frac{C_0}{R_0} = 0 \ \Rightarrow \ C_0 = 0,$$

$$w\big|_{r=R_0} = C_1 R_0 + C_{-1} R_0^{-1} = 0 \ \Rightarrow \ C_{-1} = -C_1 R_0^2.$$

Moreover, the boundary conditions (5.1) lead to the following:

$$P_0 = p_{st},\ C_1\left(r_{st} - R_0^2 r_{st}^{-1}\right) = r_{st} - R_1.$$

Therefore, we arrive at the following exact solution:

$$P = p_{st},\ w = \frac{r_{st}\,(r_{st} - R_1)}{r_{st}^2 - R_0^2}\left(r - \frac{R_0^2}{r}\right), \quad r_{st} \neq R_0. \tag{5.6}$$

In order determine the parameter r_{st}, we use the boundary condition (5.5). In the case of the above function w, condition (5.5) reduces to the following algebraic equation:

$$2(\lambda+\mu)\frac{r_{st}\,(r_{st} - R_1)}{r_{st}^2 - R_0^2} + 2\mu\frac{R_0^2\,(r_{st} - R_1)}{r_{st}(r_{st}^2 - R_0^2)} = p_a - \frac{F_0(r_{st})}{2\pi r_{st}}.$$

In the simplest case, namely $F_0 = const$, the above equation reduces to the following cubic polynomial:

$$P_3(r_{st}) \equiv \left(\lambda + \mu - \frac{p_a}{2}\right) r_{st}^3 + \left(\frac{F_0}{4\pi} - (\lambda+\mu)R_1\right) r_{st}^2 + \left(\mu + \frac{p_a}{2}\right) R_0^2 r_{st} - \left(\frac{F_0}{4\pi} + \mu R_1\right) R_0^2 = 0. \tag{5.7}$$

Therefore, depending on the coefficients, the above equation has one, two, or three real roots. Notably, $r_{st} = R_1$ if $F_0 = 2\pi R_1 p_a$.

For simplicity, we set $p_a = 0$ in what follows. Obviously, assuming $r_{st} = R_1$, one obtains $F_0 = 0$ (i.e., there is no deformation because nothing is acting on the annulus). The simplest nontrivial case occurs when $F_0 = 4\pi(\lambda + \mu)R_1$. In this case, it can be easily proven that there exists a unique positive root $r_{st} = r_*$ that belongs to the interval (R_0, R_1). Thus, one may claim that the annulus was shrinking before the steady-state arrived.

If $F_0 > 4\pi(\lambda + \mu)R_1$, then $r_* \in (R_0, R_1)$ as well. Let us prove this. The left-hand-side of (5.7) is the third-order polynomial $P_3(r_{st})$ with critical points that satisfy the following quadratic equation:

$$3(\lambda+\mu)r_{st}^2 + 2\kappa r_{st} + \mu R_0^2 = 0,$$

where $\kappa = \frac{F_0}{4\pi} - (\lambda+\mu)R_1 > 0$. By solving the above equation, one obtains the following:

$$r_{st+,-} = \frac{1}{3(\lambda+\mu)}\left(-\kappa \pm \sqrt{\kappa^2 - 3(\lambda+\mu)\mu R_0^2}\right).$$

Now, one realizes that real parts of both critical points are negative. The point r_{st-} is the point of a local maximum and r_{st+} is the point of a local minimum provided $\kappa^2 - 3(\lambda+\mu)\mu R_0^2 > 0$. Thus, the polynomial is a strictly increasing function for all $r_{st} > r_{st+}$. In the case of complex values of $r_{st\pm}$, the polynomial $P(r_{st})$ is a strictly increasing function on any interval. In both cases, the polynomial must have a real root r_*. Moreover, $r_* > r_{st+}$ if r_{st+} is a real number and r_* is a unique real root if r_{st+} is complex.

Finally, we simply calculate $P_3(R_0) = R_0^2(\lambda + 2\mu)(R_0 - R_1) < 0$ and $P_3(R_1) = \frac{F_0}{4\pi}(R_1^2 - R_0^2) > 0$; therefore, $r_* \in (R_0, R_1)$. Thus, the annulus was shrinking before the steady-state arrived.

Remark 5.1. In the case when $p_a > 0$, the situation is quite similar. By assuming $F_0 \geq 4\pi(\lambda+\mu)R_1$, it can be shown that real parts of both critical points again are negative. In this case $P_3(R_0) = R_0^2(\lambda + 2\mu)(R_0 - R_1) < 0$ and $P_3(R_1) = \left(\frac{F_0}{4\pi} - \frac{p_a R_1}{2}\right)(R_1^2 - R_0^2)$, one needs the additional restriction $F_0 > 2\pi p_a R_1$ that guaranties that the annulus shrinking (i.e., $r_* \in (R_0, R_1)$).

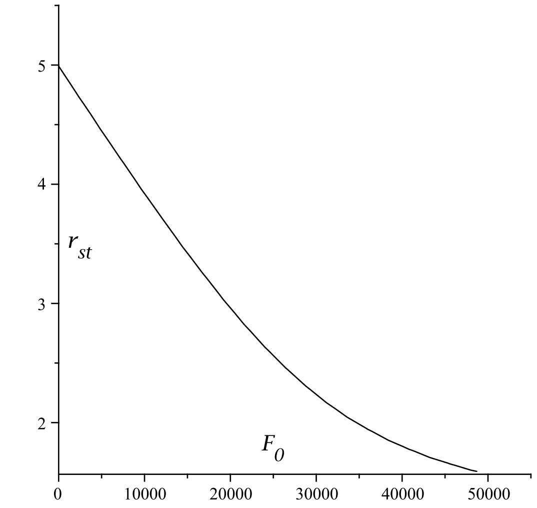

Figure 3. The curve represents the function $r_{st}(F_0)$ (see Eq (5.7) for the parameters $R_0 = 1\ mm,\ R_1 = 5\ mm,\ \lambda = 684\ mmHg,\ \mu = 15\ mHg$).

Let us present example of calculations of deformation of a tumor in the form of the annulus Ω (i.e., assuming that necrosis already started; therefore, tumor cells in the domain $\{(r,\varphi) : r < R_0\}$ are dead). We specify the parameters as follows: $R_0 = 1\ mm,\ R_1 = 5\ mm,\ \lambda = 684\ mmHg,\ \mu = 15\ mmHg$. Note that the Lame coefficients were taken from [37], while the size of the tumor can essentially vary so that average values were selected.

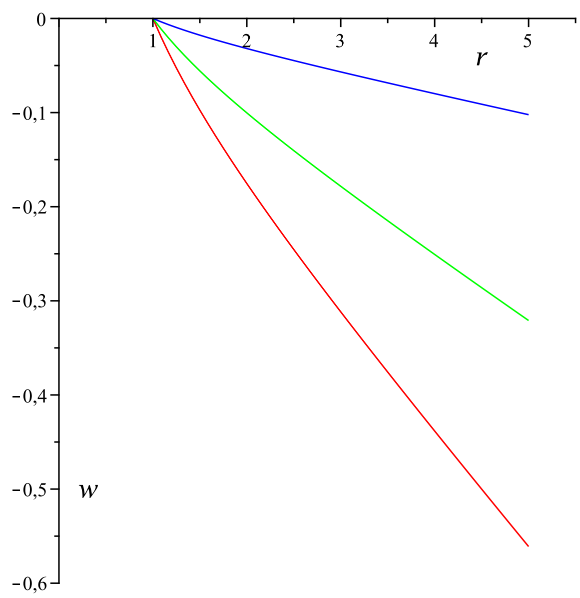

Figure 4. The curves represent deformations w (see (5.6)) for $r_{st} = 4.9\ mm$ (blue curve), $r_{st} = 4.7\ mm$ (green curve), $r_{st} = 4.5\ mm$ (red curve), and $R_0 = 1\ mm,\ R_1 = 5\ mm$.

In Figure 3, the curve represents values of r_{st} in the steady-state position of the annulus depending on the load $F_0 \geq 0$. The curve was built using the cubic equation (5.7). In Figure 4, the curves represent deformations as functions of r for three different values of r_{st}. The second formula from (5.6) was used to draw these plots. In Figure 5, the steady-state position of each circle of the radius r is presented as a function of the initial steady-state position R. We note that the second formula from (5.6) can be rewritten in the following form (see (2.2)):

$$r - R = \frac{r_{st}\,(r_{st} - R_1)}{r_{st}^2 - R_0^2}\left(r - \frac{R_0^2}{r}\right). \tag{5.8}$$

By solving the algebraic equation (5.8) with respect to the r, one easily obtains two possibilities:

$$r = \frac{R \pm \sqrt{R^2 + 4A(1 + A)R_0^2}}{2(1 + A)}.$$

Because r must be positive, we fix the upper sign as follows:

$$r = \frac{R + \sqrt{R^2 + 4A(1 + A)R_0^2}}{2(1 + A)}, \quad A = \frac{r_{st}(R_1 - r_{st})}{r_{st}^2 - R_0^2} > 0. \tag{5.9}$$

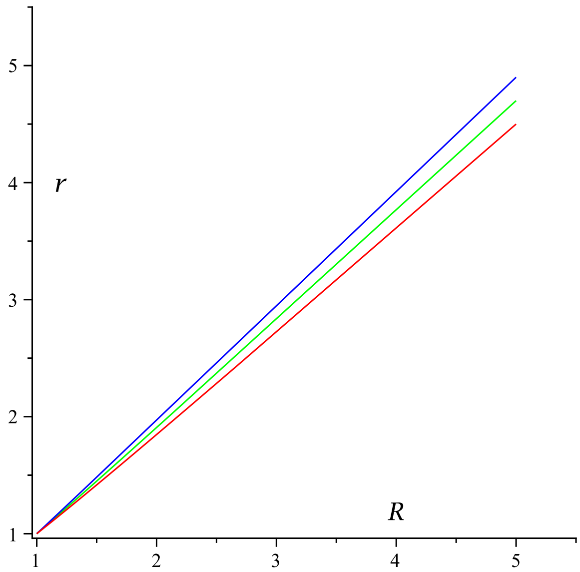

Figure 5. The curves represent the function $r(R)$ (see (5.9)) for $r_{st} = 4.9$ *mm* (blue curve), $r_{st} = 4.7$ *mm* (green curve), $r_{st} = 4.5$ *mm* (red curve), and $R_0 = 1$ *mm*, $R_1 = 5$ *mm*.

6. Conclusions

A mathematical model for PEM with the variable volume was developed in a multidimensional case. Governing equations of the model were constructed using the continuity equations, which reflect the well-known physical laws. The deformation vector was specified using the Terzaghi effective stress tensor. As a result, a model based on a system of $n + 4$ partial differential equations for unknown functions $\bar{u} = (u_1, \dots, u_n)$ (deformation vector), θ_F (porosity), ρ (density), c (concentration), and p (hydrostatic pressure) was constructed.

The model was studied in the $2D$ space approximation by analytical methods. Using the classical Lie method, it was proven that the governing equations, which form a nonlinear six-component system, admit highly nontrivial Lie symmetries leading to an infinite-dimensional Lie algebra. It was shown that the infinite-dimensional Lie algebra admits an extension in the case of PEM formed by isotropic material. Interestingly, the additional Lie symmetry is the same as for the classical Navier–Stokes equations (in the $2D$ approximation) and a model for tumor growth modeling [35, 36].

The radially-symmetric case was studied in detail. It was shown how correct boundary conditions are constructed in the case of PEM in the form of a ring that is shrinking (expanding). As a result, the BVP with a moving boundary that describes the ring deformation was constructed; additionally, the relevant BVP for the annulus deformation was presented. The nonlinear problems obtained were analytically solved in the stationary case, using the standard method to solve ODEs. In particular, the analytical formulae for unknown deformations and an unknown radius of the annulus were calculated. It was shown how deformation and an unknown radius of PEM after shrinking can be exactly calculated by relevant formulae. Illustrative plots were presented for the parameters, which are typical for tumor tissue deformation. Current research focuses on searching for time-dependent solutions of the model that admit plausible interpretations such as the stationary solutions derived in this study. Symmetry-based methods [22–24] will be applied in order to construct such solutions.

As it is shown in this study, an infinite-dimensional Lie algebra occurs for basic equations of the model. However, if one goes to boundary conditions, then this wide invariance can be broken by the geometry of the domain in question (see, a detailed discussion on this matter in [38]). Therefore, one needs to identify domains (beyond ring and annulus) in which the nonlinear PDE systems (3.1)–(3.6) still admits a nontrivial Lie symmetry. For this, an additional analysis is needed. This lies beyond the scope of this study and will be left for a future paper.

Use of AI tools declaration

The authors declare they have not used Artificial Intelligence (AI) tools in the creation of this article.

Acknowledgments

R. Cherniha is grateful to Kostas Soldatos (University of Nottingham) for useful comments. The authors are grateful to unknown reviewers for some useful comments. R. Cherniha acknowledges that this research was partly funded by the British Academy (Leverhulme Researchers at Risk Research Support Grant LTRSF-100025). V.D. acknowledges that this research was supported by a grant from the Simons Foundation (1290607, V.D.).

Conflict of interest

The authors declare there is no conflict of interest.

References

1. L. A. Taber, *Nonlinear Theory of Elasticity: Applications in Biomechanics*, World Scientific, New Jersey, 2004.
2. B. Loret, F. M. F. Simoes, *Biomechanical Aspects of Soft Tissue*, CRC Press, Boca Raton, 2017.
3. E. Detournay, A. H. D. Cheng, *Fundamentals of Poroelasticity. In: Analysis and Design Methods*, Pergamon Press, Oxford, 1993.
4. O. Coussy, *Mechanics of Porous Continua*, Wiley & Sons Ltd., New York, 1995.
5. O. Coussy, *Mechanics and Physics of Porous Solids*, Wiley & Sons Ltd., New York, 2010.
6. U. Lacis, G. A. Zampogna, S. Bagheri, A computational continuum model of poroelastic beds, *Proc. R. Soc. A: Math. Phys. Eng. Sci.*, **473** (2017), 20160932. https://doi:10.1098/rspa.2016.0932
7. J. I. Siddique, A. Ahmed, A. Aziz, C. M. Khalique, A review of mixture theory for deformable porous media and applications, *Appl. Sci.*, **7** (2017), 917. https://doi.org/10.3390/app7090917
8. V. Guerriero, S. Mazzoli, Theory of effective stress in soil and rock and implications for fracturing processes: A review, *Geosciences*, **11** (2021), 119. https://doi.org/10.3390/geosciences11030119
9. S. Speziale, S. Sivaloganathan, Poroelastic theory of transcapillary flow: Effects of endothelial glycocalyx deterioration, *Microvasc. Res.*, **78** (2009), 432–441. https://doi.org/10.1016/j.mvr.2009.07.007
10. S. Speziale, G. Tenti, S. Sivaloganathan, A poroelastic model of transcapillary flow in normal tissue, *Microvasc. Res.*, **75** (2008), 285–295. https://doi.org/10.1016/j.mvr.2007.07.001
11. F. Travascio, R. Serpieri, S. Asfour, Articular cartilage biomechanics modeled via an intrinsically compressible biphasic model: Implications and deviations from an incompressible biphasic approach, in *Proceedings of the ASME 2013 Summer Bioengineering Conference*, 2013. https://doi.org/10.1115/SBC2013-14082
12. P. Mascheroni, M. Carfagna, A. Grillo, D. P. Boso, B. A. Schrefler, An avascular tumor growth model based on porous media mechanics and evolving natural states, *Math. Mech. Solids.*, **23** (2018), 686–712. https://doi.org/10.1177/1081286517711217
13. D. R. Sowinski, M. D. McGarry, E. E. Van Houten, S. Gordon-Wylie, J. B. Weaver, K. D. Paulsen, Poroelasticity as a model of soft tissue structure: Hydraulic permeability reconstruction for magnetic resonance elastography in silico, *Front Phys.*, **8** (2021), 617582. https://doi.org/10.3389/fphy.2020.617582
14. R. Cherniha, J. Stachowska-Pietka, J. Waniewski, A mathematical model for transport in poroelastic materials with variable volume: Derivation, lie symmetry analysis, and examples, *Symmetry*, **12** (2020), 396. https://doi.org/10.3390/sym12030396
15. R. Cherniha, V. Davydovych, J. Stachowska-Pietka, J. Waniewski, A mathematical model for transport in poroelastic materials with variable volume: Derivation, Lie symmetry analysis and examples–Part 2, *Symmetry*, **14** (2022), 109. https://doi.org/10.3390/sym14010109
16. R. Cherniha, J. Stachowska-Pietka, J. Waniewski, A mathematical model for two solutes transport in a poroelastic material and its applications, *Commun. Nonlinear Sci. Numer. Simulat.*, **132** (2024), 107905. https://doi.org/10.1016/j.cnsns.2024.107905

17. E. Samaniego, C. Anitescu, S. Goswami, V. M. Nguyen-Thanh, H. Guo, K. Hamdia, et al., An energy approach to the solution of partial differential equations in computational mechanics via machine learning: Concepts, implementation and applications, *Comput. Methods Appl. Mech. Eng.*, **362** (2020), 112790. https://doi.org/10.1016/j.cma.2019.112790
18. K. P. Soldatos, On the bending problem of a polar linearly elastic cantilever, *Mech. Res. Commun.*, **147** (2025), 104448. https://doi.org/10.1016/j.mechrescom.2025.104448
19. R. Cherniha, V. Davydovych, A. Vorobyova, New Lie symmetries and exact solutions of a mathematical model describing solute transport in poroelastic materials, *Math. Comp. Appl.*, **29** (2024), 43. https://doi.org/10.3390/mca29030043
20. D. A. Narmoneva, J. Y. Wang, L. A. Setton, A noncontacting method for material property determination for articular cartilage from osmotic loading, *Biophy. J.*, **81** (2001), 3066–3076. https://doi.org/10.1016/S0006-3495(01)75945-0
21. P. Li, M. Schanz, Wave propagation in a 1-D partially saturated poroelastic column, *Geophys. J. Int.*, **184** (2011), 1341–1353. https://doi.org/10.1111/j.1365-246X.2010.04913.x
22. G. W. Bluman, A. F. Cheviakov, S. C. Anco, *Applications of Symmetry Methods to Partial Differential Equations*, Springer, New York, 2010.
23. D. J. Arrigo, *Symmetry Analysis of Differential Equations*, John Wiley & Sons, Hoboken, 2015.
24. R. Cherniha, M. Serov, O. Pliukhin, *Nonlinear Reaction-Diffusion-Convection Equations: Lie and Conditional Wymmetry, Exact Solutions and Their Applications*, CRC Press, Boca Raton, 2018.
25. S. Mandal, S. Ghosh, Modelling and nonclassical symmetry analysis of a complex porous media flow in a dilating channel, *Physica D*, **481** (2025), 134834. https://doi.org/10.1016/j.physd.2025.134834
26. R. Cherniha, Comments on the paper Modelling and nonclassical symmetry analysis of a complex porous media flow in a dilating channel, preprint, arXiv:2511.08656.
27. R. Cherniha, V. Davydovych, A hunter-gatherer-farmer population model: Lie symmetries, exact solutions and their interpretation, *Euro. J. Appl. Math.*, **30** (2019), 338–357. https://doi.org/10.1017/S0956792518000104
28. E. Alimirzaluo, M. Nadjafikhah, J. Manafian, Some new exact solutions of (3 + 1)-dimensional Burgers system via Lie symmetry analysis, *Adv. Differ. Equ.*, **2021** (2021), 60. https://doi.org/10.1186/s13662-021-03220-3
29. R. Cherniha, V. Davydovych, A hunter-gatherer-farmer population model: New conditional symmetries and exact solutions with biological interpretation, *Acta Appl. Math.*, **182** (2022), 4. https://doi.org/10.1007/s10440-022-00537-3
30. A. Paliathanasis, Symmetry analysis for the 2D Aw-Rascle traffic-flow model of multi-lane motorways in the Euler and Lagrange variables, *Symmetry*, **15** (2023), 1525. https://doi.org/10.3390/sym15081525
31. S. Shagolshem, B. Bira, S. Sil, Application of symmetry analysis to viscoelastic fluid model, *Commun. Nonlinear. Sci. Numer. Simulat.*, **125** (2023), 107417. https://doi.org/10.1016/j.cnsns.2023.107417

32. M. Gorgone, F. Oliveri, E. Sgroi, Hierarchy of coupled Burgers-like equations induced by conditional symmetries, *Z. Angew. Math. Phys.*, **76** (2025), 8. https://doi.org/10.1007/s00033-024-02405-6

33. K. Terzaghi, Relation between soil mechanics and foundation engineering, in *Proceedings of the International Conference on Soil Mechanics and Foundation Engineering*, (1936), 13–18.

34. R. Cherniha, J. Stachowska-Pietka, J. Waniewski, A mathematical model for fluid-glucose-albumin transport in peritoneal dialysis, *Int. J. Appl. Math. Comput. Sci.*, **24** (2014), 837–851. https://doi.org/10.2478/amcs-2014-0062

35. S. P. Lloyd, The infinitesimal group of the Navier–Stokes equations, *Acta Mech.*, **38** (1981), 83–98. https://doi.org/10.1007/BF01351464

36. R. Cherniha, V. Davydovych, Lie symmetries, reduction and exact solutions of the (1 + 2)-dimensional nonlinear problem modeling the solid tumour growth, *Commun. Nonlinear. Sci. Numer. Simulat.*, **80** (2020), 104980. https://doi.org/10.1016/j.cnsns.2019.104980

37. P. A. Netti, L. T. Baxter, Y. Boucher, R. Skalak, R. K. Jain, Macro- and microscopic fluid transport in living tissues: Application to solid tumors, *AIChE J.*, **3** (1997), 818–834. https://doi.org/10.1002/aic.690430327

38. R. Cherniha, J. R. King, Lie and conditional symmetries of a class of nonlinear (1 + 2)-dimensional boundary value problems, *Symmetry*, **7** (2015), 1410–1435. https://doi.org/10.3390/sym7031410